Interaction parameters for blends containing polycarbonates: 1. Tetramethyl bisphenol-A polycarbonate/polystyrene

C. K. Kim and D. R. Paul*
Department of Chemical Engineering and Center for Polymer Research, University of Texas at Austin, Austin, TX 78712, USA
(Received 25 March 1991; accepted 28 April 1991)

The interaction parameters for polystyrene and tetramethyl bisphenol-A polycarbonate blends were evaluated by fitting experimental *PVT* behaviour and a lower critical solution temperature (LCST)-type phase boundary to the lattice fluid theory of Sanchez and Lacombe. The phase boundaries of these blends were obtained by using a differential scanning calorimetry (d.s.c.) method, and were compared with those obtained by light transmission and visual methods. The characteristic properties for these polymers were determined by the non-linear least-squares fitting of specific volume data as a function of temperature and pressure to the equation of state. The net bare interaction parameters from the Sanchez–Lacombe theory, ΔP^*, calculated at several compositions yielded negative values ($\Delta P^* = -0.17 \pm 0.01$ cal cm^{-3}) and did not depend on composition. Flory–Huggins type interaction parameters reported in the literature for this system determined by a small-angle neutron scattering technique compare favourably with the results of this study except in terms of composition dependence.

(Keywords: blends; tetramethyl polycarbonate; polystyrene; LCST; equation of state)

INTRODUCTION

Blends of polystyrene, PS, and tetramethyl bisphenol-A polycarbonate, TMPC, have been studied extensively[1–9]. The miscibility of PS and TMPC was first suggested by Shaw[1]. Subsequently glass transition behaviour and a phase diagram for this system were reported by Casper and Morbitzer[2]. Other authors[4–6] have presented results of density, thermal analysis and mechanical measurements for PS/TMPC blends. Neutron scattering results have been reported[7,8] that provide some information about the interaction parameter for this system. More recently, Guo and Higgins[9] reported the effect of PS molecular weight on the LCST behaviour of blends with TMPC determined by light scattering and microscopy methods.

Some time ago this laboratory became interested in blends of TMPC with other polymers[6,10,11], and this paper is the first in a series aimed at extending and refining these earlier observations. One of the objectives is quantitatively to evaluate the interaction parameters responsible for the equilibrium phase behaviour in these systems. This information will be obtained by analysis of the phase diagram by using models for the free energy of mixing, particularly the lattice fluid theory of Sanchez and Lacombe[12–16]. This strategy requires pressure–volume–temperature (*PVT*) data for each polymeric component so that equation-of-state parameters can be determined in addition to an accurate liquid–liquid phase diagram. This paper focuses on the use of this approach to determine interaction energies for the base system TMPC and PS; whereas, subsequent papers will deal with related copolymers.

MATERIALS AND PROCEDURES

TMPC was supplied by Bayer AG, and its weight-average molecular weight determined by light-scattering measurements in this laboratory is $\bar{M}_w = 33\,000$ g mol^{-1}. TMPC has a rather high glass transition temperature and is resistant to hydrolysis because of methyl substitution on the phenyl ring. The PS was Cosden 550 from Cosden Oil and Chem. Co, which has $\bar{M}_w = 330\,000$ g mol^{-1} and $\bar{M}_n = 100\,000$ g mol^{-1}. Blends of TMPC and PS were prepared by casting solutions containing 5% total polymer in tetrahydrofuran onto a glass plate mounted on a heating block at 50–60°C for 5 min. The blends were finally dried in a vacuum oven at 130–140°C for a week. Thermal analysis showed that this procedure effectively removed the solvent.

Glass transition temperatures and other thermal characteristics were determined with a Perkin–Elmer DSC-7 system. The first scan was run to 220°C to erase previous thermal history during sample preparation and storage, then the sample was quenched to 25°C to start the second scan. The onset of the transition in heat capacity was defined as the glass transition temperature.

The temperature at which phase separation caused by LCST behaviour occurred was measured by visual and light transmission techniques and a d.s.c. method to assess the closest possible approximation to true equilibrium. For the visual technique, the specimen was covered with a glass slide on a hot plate and heated until it became cloudy. To reduce the possibility of thermal decomposition, the film was heated rapidly to a temperature about 20°C below the expected cloud point and then heated at 2°C min^{-1} to the cloud point and beyond. The temperature at which the blends first started to transform from transparent to cloudy by visual assess-

* To whom correspondence should be addressed

0032-3861/92/081630-10

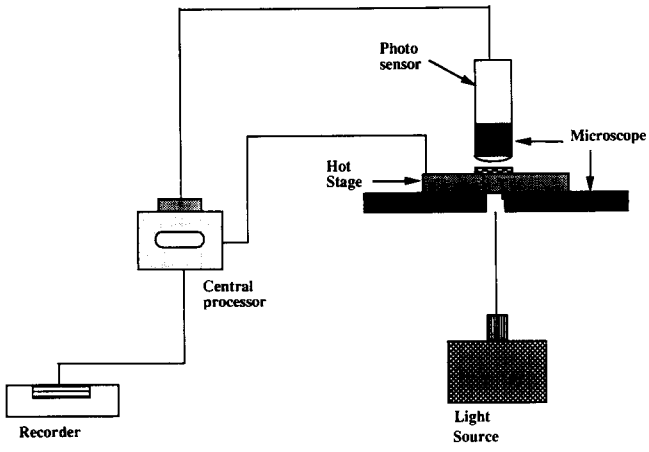

Figure 1 Schematic illustration of light transmission equipment for cloud-point measurement. The optical microscope was equipped with a 4 × objective lens and the photosensor replaced the lens of the eyepiece

ment was taken as the cloud point. Optical cloud points were also determined by quantitative measurement of the light transmission through a specimen mounted on a hot stage (Mettler FP 82 HT) equipped with a temperature controller (Mettler FP 80 HT).

Figure 1 shows a schematic diagram of the light transmission equipment. Changes in transmitted light intensity were recorded at a wavelength of 600 nm as the specimens were heated at a scanning rate of 2°C min^{-1}. The temperature at which the light intensity first started to change was taken as the cloud point. The d.s.c. method relied on changes in glass transition behaviour rather than optical changes. Blend specimens were annealed in the d.s.c. at fixed temperatures close to the expected phase boundary for specified periods of time, after which they were quenched to room temperature. D.s.c. scans were then run to determine whether or not a change from one glass transition to two had occurred as a result of the annealing.

The density of TMPC and PS were determined by a density gradient column operated at 30°C. The changes in specific volume as a function of temperature and pressure were measured with a Gnomix *PVT* apparatus. For isothermal operation, samples were compressed along 31 isotherms, from 30°C up to about 290°C, with volume data recorded at presure intervals of 10 MPa between 10 and 200 MPa. These data were fitted to the Tait equation and the volume at zero pressure for each isothermal was obtained by extrapolation. For isobaric operation, TMPC was heated from 30°C to 290°C at 2.5°C min^{-1} at several fixed pressures.

BACKGROUND

The free energy of mixing per unit volume, g, can be expressed in terms of the classical Flory–Huggins theory:

$$\Delta g_m = \Delta g_{nc} + \Delta g_c \quad (1)$$

where Δg_c is the combinatorial entropy[17,18]

$$\Delta g_c = RT\left(\frac{\phi_1 \ln \phi_1}{\tilde{V}_1} + \frac{\phi_2 \ln \phi_2}{\tilde{V}_2}\right) \quad (2)$$

and Δg_{nc} is the non-combinatorial free energy represented by the Van-Laar form[19]

$$\Delta g_{nc} = B\phi_1\phi_2 \quad (3)$$

The ϕ_i and $\tilde{V}_i$ are the volume fraction and molar volume of component i, respectively, and B is the interaction energy density. The combinatorial entropy always favours mixing. If the interaction parameter is negative then, according to this theory, all binary compositions are miscible at all temperatures. When B is independent of temperature, this theory only predicts upper critical solution temperature (UCST)-type behaviour. If B is a function of temperature, basic thermodynamic relations reveal that this quantity is not strictly an enthalpic parameter, but also contains a non-combinatorial entropic contribution. An empirical excess entropy term $-TS^E = -TB^s\phi_1\phi_2$ is often added to equation (1), which enables the theory to describe LCST behaviour. In this extended Flory–Huggins theory, the interaction parameter takes on the form

$$B(T) = B^h - TB^s \quad (4)$$

If the interaction energy density in equation (3) does not depend on ϕ_i, simple differentiation of equations (1)–(3) leads to the familiar spinodal condition

$$\frac{d^2\Delta g}{d\phi_1^2} = RT\left(\frac{1}{\phi_1\tilde{V}_1} + \frac{1}{\phi_2\tilde{V}_2}\right) - 2B_{sc} = 0 \quad (5)$$

This form is often used even though the interaction energy does depend on ϕ_1. Thus, equation (5) amounts to the definition of a new interaction energy, i.e.

$$B_{sc} = -\frac{1}{2}\frac{d^2\Delta g_{nc}}{d\phi_1^2} \quad (6)$$

to which the subscript sc is added, following the notation of Sanchez[20], in order to distinguish it from B in equation (3). In general, interaction energies defined by equations (1)–(3), equation (5) or other free-energy-derived equations are not identical, but are interrelated as shown by Sanchez[20], e.g.

$$B_{sc} = B(T) + (\phi_1 - \phi_2)\frac{dB(T)}{d\phi_1} - \tfrac{1}{2}\phi_1\phi_2\frac{d^2B(T)}{d\phi_1^2} \quad (7)$$

The interaction parameters used here have units of energy/volume and differ by the factor kT from the χ quantities used by Sanchez[20].

The extended Flory–Huggins theory ignores the fact that the mixture is compressible. Equation of state theories have emerged to account for this effect and they predict LCST behaviour without resorting to the empiricism used in equation (4). These theories can be forced into the Flory–Huggins form to obtain their predicted expressions for B, B_{sc} and the other interaction parameters described by Sanchez[20]. These expressions naturally depend on temperature and composition. It is appealing to attribute the experimentally observed temperature and composition dependence of the Flory–Huggins-type interaction parameters to equation-of-state-type effect, and that is an assumption that we make here. However, it should be recognized that other mechanisms could contribute to the dependence on T and ϕ. There are several equation of state theories[21–25] for mixtures, but the following discussion is limited to the lattice fluid theory of Sanchez and Lacombe[12–16]. This theory expresses thermodynamic functions in terms of reduced variables $\tilde{P} = P/P^*$, $\tilde{T} = T/T^*$, $\tilde{\rho} = 1/\tilde{v} = \rho/\rho^* = v_{sp}^*/v_{sp}$ where the asterisks denote characteristic parameters. The free energy per unit hard core volume

is given by

$$\frac{G}{rv^*} = \frac{G}{V^*} = g_{nc} + g_c \tag{8}$$

where

$$g_{nc} = -\tilde{\rho}P^* + P\tilde{v} + \frac{RT}{v^*}\left(\frac{1-\tilde{\rho}}{\tilde{\rho}}\ln(1-\tilde{\rho}) + \frac{\ln\tilde{\rho}}{r}\right) \tag{9}$$

and

$$g_c = \frac{RT}{v^*}\sum_i \frac{\phi_i}{r_i}\ln\phi_i \tag{10}$$

Chain length, r, is given by $r = MP^*/RT^*\rho^*$, where M is the molecular weight (weight average should be used for polydisperse components). The enthalpy of mixing ΔH_m at low pressure for a binary mixture is given by

$$\frac{\Delta H_m}{V} = \tilde{\rho}^2\,\Delta P^*\phi_1\phi_2 + \tilde{\rho}[\phi_1 P_1^*(\tilde{\rho}_1 - \tilde{\rho}) + \phi_2 P_2^*(\tilde{\rho}_2 - \tilde{\rho})] \tag{11}$$

The characteristic pressure for the mixture, P^*, is related to those of the pure components, P_i^*, and the bare interaction energy, ΔP^*, by

$$P^* = \phi_1 P_1^* + \phi_2 P_2^* - \phi_1\phi_2\,\Delta P^* \tag{12}$$

where the ϕ_i are close-packed volume fractions. The reduced density $\tilde{\rho}$ refers to the mixture, whereas $\tilde{\rho}_i$ refers to the pure components. Equation (11) allows for the effects of finite compressibility on the enthalpy of mixing. Interaction parameters defined in the extended Flory–Huggins theory can be simply expressed in terms of the equation of state parameters by assuming the ϕ_i used in the two theories are essentially equal. From equations (4) and (11), the interaction energy related to the heat of mixing, B^h, is given by

$$B^h = \tilde{\rho}\,\Delta P^* + \left[\frac{P_1^*}{\phi_2}(\tilde{\rho}_1 - \tilde{\rho}) + \frac{P_2^*}{\phi_1}(\tilde{\rho}_2 - \tilde{\rho})\right] \tag{13}$$

A relationship for the excess entropy term, $-TB^s$, can be similarly derived

$$-TB^s = \frac{RT}{\phi_1\phi_2}\left\{\frac{1}{v^*}\left[\frac{1-\tilde{\rho}}{\tilde{\rho}}\ln(1-\tilde{\rho}) + \frac{\ln\tilde{\rho}}{r}\right] - \frac{\phi_1}{v_1^*}\left[\frac{1-\tilde{\rho}_1}{\tilde{\rho}_1}\ln(1-\tilde{\rho}_1) + \frac{\ln\tilde{\rho}_1}{r_1^0}\right] - \frac{\phi_2}{v_2^*}\left[\frac{1-\tilde{\rho}_2}{\tilde{\rho}_2}\ln(1-\tilde{\rho}_2) + \frac{\ln\tilde{\rho}_2}{r_2^0}\right]\right\} \tag{14}$$

Finally, the spinodal condition for a compressible mixture can be written[26]

$$\frac{d^2g}{d\phi^2} = g_{\phi\phi} - \frac{(g_{\tilde{\rho}\phi})^2}{g_{\tilde{\rho}\tilde{\rho}}} = 0 \tag{15}$$

where the subscripts ϕ and $\tilde{\rho}$ indicate partial derivatives with respect to ϕ or $\tilde{\rho}$. From equations (6) and (15), the following expression for B_{sc} is obtained

$$B_{sc} = \tilde{\rho}\,\Delta P^* + \left\{[P_2^* - P_1^* + (\phi_2 - \phi_1)\,\Delta P^*] + \frac{RT}{\tilde{\rho}}\left(\frac{1}{r_1^0 v_1^*} - \frac{1}{r_2^0 v_2^*}\right) - RT\left(\frac{\ln(1-\tilde{\rho})}{\tilde{\rho}^2} + \frac{1}{\tilde{\rho}}\right)\left(\frac{1}{v_1^*} - \frac{1}{v_2^*}\right)\right\}^2 \Bigg/ \left\{\frac{2RT}{v^*}\left[\frac{2\ln(1-\tilde{\rho})}{\tilde{\rho}^3} + \frac{1}{\tilde{\rho}^2(1-\tilde{\rho})} + \frac{(1-1/r)}{\tilde{\rho}^2}\right]\right\} \tag{16}$$

RESULTS AND DISCUSSION

PVT behaviour

Figure 2 shows representative *PVT* behaviour of TMPC obtained from isobaric experiments. From these results, the pressure dependence of T_g, defined as the intersection of the isobars above and below the transition region (line in *Figure 2*), was obtained. As shown in *Figure 3*, T_g increases linearly with pressure according to the equation

$$T_g(p) = 185.8 + 0.667p \tag{17}$$

where T is in degrees Celsius and p is in megapascals. The small dips in volume just below T_g at high pressures have been noted by others[27–29] and may stem from volume relaxations on the time-scale of the experiment when the formation pressure of the sample is lower than the experimental pressure. Specific volumes of pure TMPC and PS above the T_g obtained from isothermal experiments are listed in *Table 1* and *Table 2*. These were fitted to the Tait equation[30–32]

$$V(p, T) = V(0, T)\{1 - 0.0894\ln[1 + p/C(T)]\} \tag{18}$$

by regression analysis, where $V(p, T)$ is the specific volume ($cm^3\,g^{-1}$) at pressure p(bar) and temperature T(°C). The term $V(0, T)$ is the specific volume at zero pressure. The temperature dependence of $V(0, T)$ and $C(T)$ are represented by the forms

$$C(T) = C_0\exp(-b_1T) \tag{19}$$

$$V(0, T) = a_0 + a_1T + a_2T^2 \tag{20}$$

Table 3 lists these parameters for TMPC and PS in the

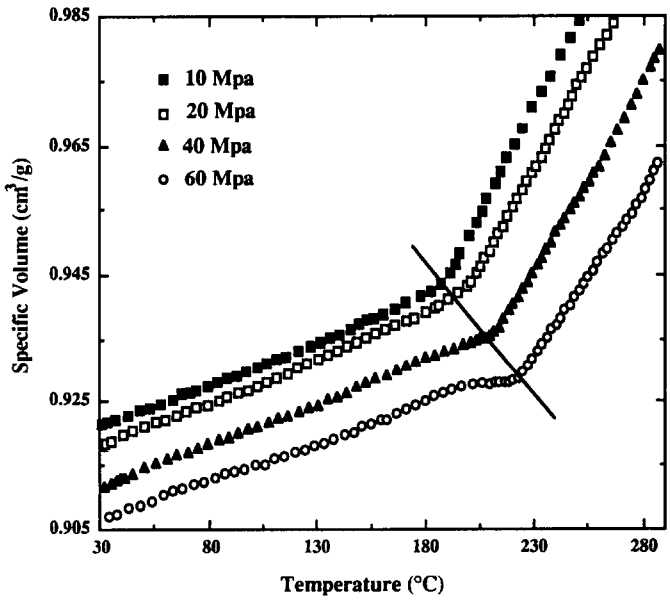

Figure 2 Change in specific volume of TMPC as a function of temperature and pressure

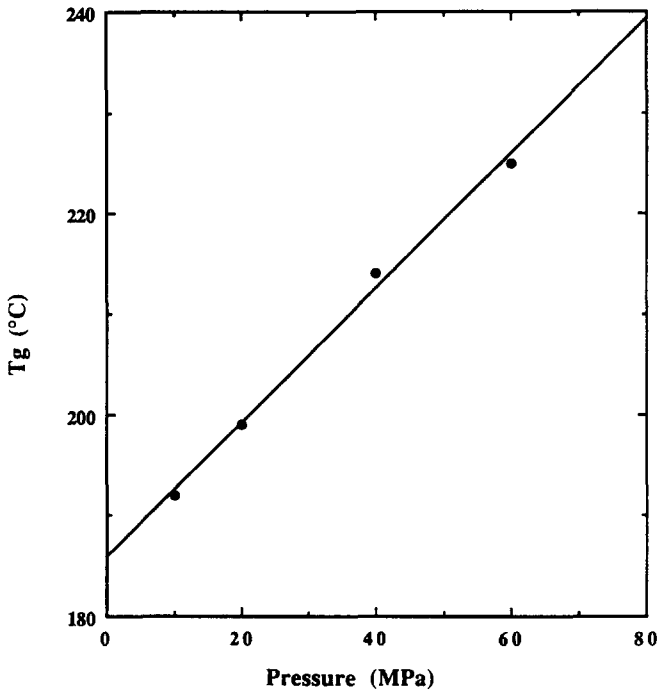

Figure 3 The glass transition temperature of TMPC obtained from the isobaric volume–temperature plots in *Figure 2*

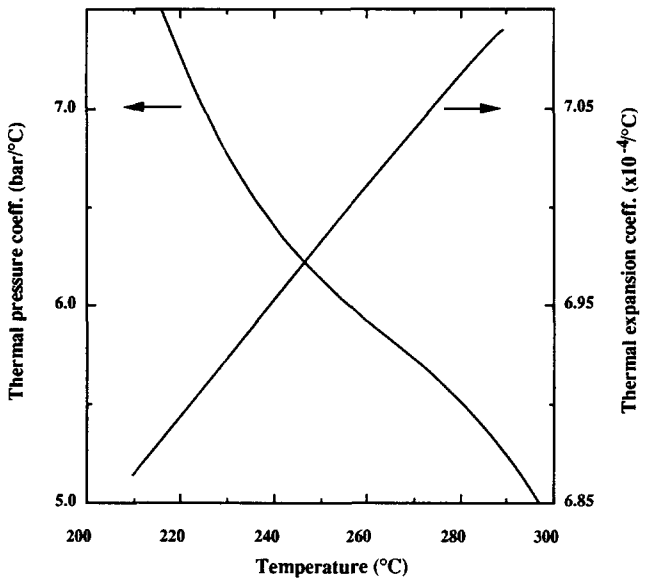

Figure 4 Thermal expansion and thermal pressure coefficients of TMPC at zero pressure calculated from the Tait equation

glassy and liquid states. The constants for PS are in good agreement with other published results[33,34]. *Figure 4* shows the thermal expansion and thermal pressure coefficients of TMPC computed from the Tait equation at zero pressure.

Characteristic parameters

For each pure component, the experimental $V(T, p)$ data can be fitted to the theoretical equation of state by non-linear regression to yield a set of characteristic parameters that best represent the data over the temperature and pressure ranges considered[13]. While the equation of state proposed by Sanchez and Lacombe has a simpler and more convenient closed mathematical form than many others, it shows systematic deviations in the regression at high pressure[35,36]. Thus, only low-pressure data where this is not a problem were used. To some extent the characteristic parameters obtained depend on temperature, so for most reliable results the same temperature range should be used for both polymers[37]. *Table 3* lists the characteristic parameters for TMPC and PS obtained from the pressure and temperature region 0–50 MPa and 220–270°C. The latter includes the range where phase separation of TMPC/PS blends occurs.

Thermal behaviour

Figure 5 shows the T_g behaviour of blends prepared by the hot casting method. A single intermediate T_g is observed at all compositions as reported by others[4,6,9].

On heating, these blends turned cloudy due to phase separation. The phase separation temperature was estimated by a simple visual technique, by a quantitative light transmission method, and by monitoring T_g behaviour by d.s.c. after heat treatment. *Figure 6* compares the phase separation temperatures obtained by these methods. The results using the simple visual method are higher than those obtained by the other two approaches. One source of error in the former is a slight difference in temperature between the thermal sensor and the sample owing to heat transfer effects inherent in this apparatus. The data by the d.s.c. method are believed to be the most reliable because rate effects were effectively eliminated, and these results were used to calculate the interaction energies.

Figure 7 shows d.s.c. thermograms for a blend containing 50 wt% of PS after annealing at 235°C for 5 min (curve a) and at 265°C for 5 min (curve b). After each heating step, the samples were rapidly quenched such that any phase separation that occurred did not

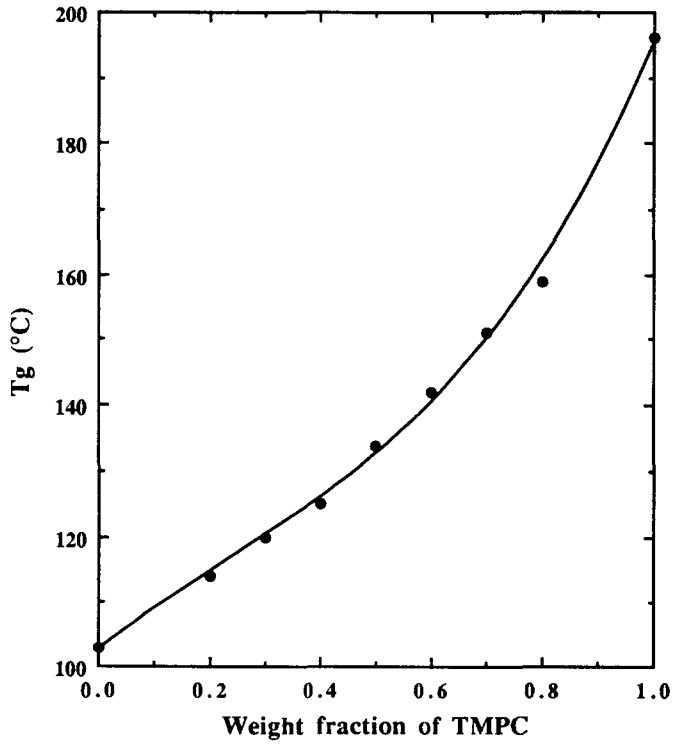

Figure 5 Glass transition temperature behaviour of TMPC/PS blends determined by d.s.c. at 20°C min^{-1} by using the onset method

Table 1 Specific volume ($cm^3\ g^{-1}$) of TMPC as a function of temperature and pressure in the liquid state

T (°C)	P (MPa) = 0	10	20	30	40	50	60	70	80	90	100	110	120	130	140	150	160	170	180	190
218.4	0.9787	0.9700	0.9612	0.9545	0.9481	0.9423	0.9372	–	–	–	–	–	–	–	–	–	–	–	–	–
224.6	0.9837	0.9746	0.9657	0.9588	0.9522	0.9460	0.9402	0.9354	–	–	–	–	–	–	–	–	–	–	–	–
233.5	0.9912	0.9811	0.9709	0.9637	0.9546	0.9500	0.9441	0.9385	–	–	–	–	–	–	–	–	–	–	–	–
241.6	0.9961	0.9858	0.9753	0.9677	0.9604	0.9542	0.9479	0.9423	–	–	–	–	–	–	–	–	–	–	–	–
251.0	1.0016	0.9911	0.9811	0.9727	0.9658	0.9588	0.9523	0.9467	0.9411	0.9359	–	–	–	–	–	–	–	–	–	–
253.2	1.0050	0.9937	0.9821	0.9740	0.9665	0.9601	0.9536	0.9477	0.9422	0.9371	–	–	–	–	–	–	–	–	–	–
262.6	1.0091	0.9978	0.9870	0.9782	0.9706	0.9636	0.9570	0.9509	0.9454	0.9402	0.9352	–	–	–	–	–	–	–	–	–
266.6	1.0124	1.0007	0.9893	0.9804	0.9724	0.9658	0.9590	0.9534	0.9473	0.9416	0.9367	0.9323	–	–	–	–	–	–	–	–
271.5	1.0149	1.0033	0.9923	0.9837	0.9753	0.9681	0.9613	0.9550	0.9492	0.9439	0.9390	0.9342	0.9298	–	–	–	–	–	–	–
276.3	0.0171	1.0058	0.9943	0.9853	0.9771	0.9700	0.9631	0.9569	0.9511	0.9457	0.9403	0.9356	0.9311	0.9267	–	–	–	–	–	–
280.6	1.0212	1.0090	0.9978	0.9885	0.9802	0.9726	0.9655	0.9590	0.9531	0.9480	0.9427	0.9377	0.9330	0.9285	0.9244	0.9200	0.9159	–	–	–
285.0	0.0250	0.0125	1.0005	0.9911	0.9827	0.9750	0.9680	0.9613	0.9555	0.9500	0.9452	0.9398	0.9351	0.9305	0.9257	0.9217	0.9174	0.9134	0.9091	–
289.6	1.0306	1.0175	1.0050	0.9951	0.9868	0.9791	0.9717	0.9647	0.9584	0.9527	0.9475	0.9424	0.9373	0.9326	0.9282	0.9238	0.9193	0.9151	0.9111	0.9069

Table 2 Specific volume ($cm^3\ g^{-1}$) of PS as a function of temperature and pressure in the liquid state

T (°C)	P (MPa) = 0	10	20	30	40	50	60	70	80	90	100	110	120	130	140	150	160	170	180	190
113.9	0.9729	0.9672	–	–	–	–	–	–	–	–	–	–	–	–	–	–	–	–	–	–
127.9	0.9801	0.9738	0.9676	0.9623	0.9575	0.9527	–	–	–	–	–	–	–	–	–	–	–	–	–	–
141.3	0.9872	0.9805	0.9740	0.9684	0.9633	0.9584	0.9538	0.9493	0.9452	0.9413	–	–	–	–	–	–	–	–	–	–
154.7	0.9949	0.9877	0.9807	0.9749	0.9695	0.9643	0.9595	0.9548	0.9504	0.9467	0.9428	–	–	–	–	–	–	–	–	–
167.7	1.0021	0.9946	0.9874	0.9812	0.9755	0.9702	0.9652	0.9604	0.9559	0.9517	0.9477	0.9439	0.9403	0.9368	–	–	–	–	–	–
181.0	1.0100	1.0020	0.9942	0.9879	0.9819	0.9763	0.9709	0.9660	0.9614	0.9572	0.9530	0.9491	0.9452	0.9416	0.9381	0.9347	0.9312	0.9280	0.9248	0.9216
193.9	1.0173	1.0090	1.0010	0.9943	0.9881	0.9824	0.9770	0.9718	0.9669	0.9624	0.9579	0.9540	0.9502	0.9464	0.9427	0.9392	0.9356	0.9322	0.9290	0.9255
206.9	1.0250	1.0162	1.0077	1.0006	0.9941	0.9881	0.9825	0.9770	0.9720	0.9673	0.9628	0.9588	0.9549	0.9509	0.9470	0.9434	0.9399	0.9363	0.9328	0.9295
219.5	1.0325	1.0232	1.0142	1.0069	1.0001	0.9939	0.9878	0.9824	0.9771	0.9724	0.9678	0.9635	0.9594	0.9553	0.9517	0.9478	0.9440	0.9405	0.9369	0.9333
232.7	1.0410	1.0310	1.0212	1.0134	1.0062	0.9998	0.9936	0.9878	0.9823	0.9773	0.9727	0.9683	0.9641	0.9598	0.9559	0.9519	0.9481	0.9445	0.9406	0.9370
245.6	1.0488	1.0383	1.0279	1.0200	1.0126	1.0058	0.9991	0.9932	0.9875	0.9824	0.9776	0.9732	0.9686	0.9645	0.9604	0.9563	0.9523	0.9486	0.9447	0.9410
258.5	1.0574	1.0459	1.0349	1.0263	1.0184	1.0114	1.0046	0.9984	0.9925	0.9872	0.9821	0.9774	0.9729	0.9683	0.9644	0.9601	0.9560	0.9520	0.9482	0.9443

Table 3 Summary of the TMPC and PS parameters for the Tait equation and the Sanchez–Lacombe equation of state

	TMPC	PS
Glass		
Temperature range (°C)	30–170	30–90
a_0 ($cm^3\ g^{-1}$)	0.9180	0.9530
a_1 ($cm^3\ g^{-1}\ °C^{-1}$)	1.2086×10^{-4}	9.9909×10^{-6}
a_2 ($cm^3\ g^{-1}\ °C^{-2}$)	7.4217×10^{-9}	1.1335×10^{-6}
C_0 (bar)	3188	3702
b_1 ($°C^{-1}$)	1.9572×10^{-3}	4.8811×10^{-3}
Liquid		
Temperature range (°C)	210–290	110–270
a_0 ($cm^3\ g^{-1}$)	0.8497	0.91902
a_1 ($cm^3\ g^{-1}\ °C^{-1}$)	5.0727×10^{-4}	4.2281×10^{-4}
a_2 ($cm^3\ g^{-1}\ °C^{-2}$)	3.8318×10^{-7}	4.3317×10^{-7}
C_0 (bar)	2314	2236
b_1 ($°C^{-1}$)	4.2419×10^{-3}	3.841×10^{-3}
Temperature range (°C)	220–270	220–270
T^* (K)	729	810
P^* (bar)	4395	3809
ρ^* ($g\ cm^{-3}$)	1.1854	1.0922
r^0	2018	17083

Note: $r^0 = MP^*/RT^*\rho^*$ when M is the weight-average molecular weight

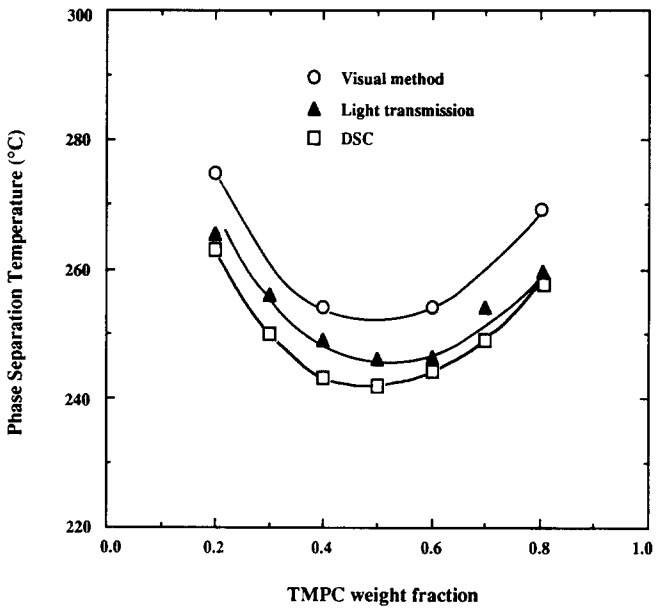

Figure 6 Comparison of phase separation temperatures of TMPC/PS blends obtained by using three different methods

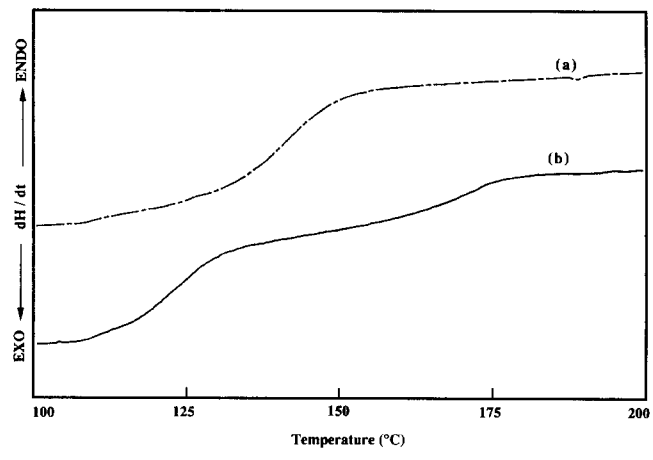

Figure 7 D.s.c. thermograms for a TMPC/PS blend containing 50 wt% PS: (a) after annealing at 235°C for 5 min; (b) after annealing at 265°C for 5 min

have time to be reversed on cooling. The sample heated at 235°C retains the single T_g of a homogeneous blend while the sample heated at 265°C shows two T_gs, indicating that phase separation occurred. Obviously the phase boundary would appear to lie between 235°C and 265°C for this composition. Whether this is indeed an equilibrium phase boundary can be assessed by examining reversibility of the phase separation[38]. The thermal programme used to test for reversibility is illustrated in *Figure 8* while *Figure 9* shows sample d.s.c. thermograms obtained for a blend containing 40 wt% of PS. Curve a in *Figure 9* is a second scan after a first scan to just above T_g for erasing prior thermal history for the as-prepared blend. A single T_g is seen as expected. The first annealing step was done at $T_1 = 255°C$ (for 5 min). This is above the phase separation temperature, so afterwards the blend has two T_gs as shown in curve b. Next, this sample was annealed again for 1 h at $T_2 = 235°C$, which is just below the phase boundary. The sample was quenched again to room temperature, after which the last d.s.c. scan was performed. The glass transition behaviour for this last scan (curve c) is exactly the same as that in curve a. From this, we see that the phase separation induced at 255°C can be reversed at 235°C; thus, the

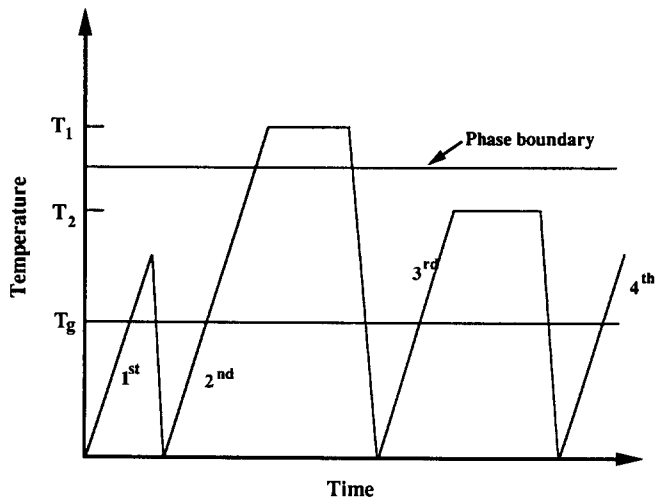

Figure 8 Thermal programme used to test reversibility of phase separation

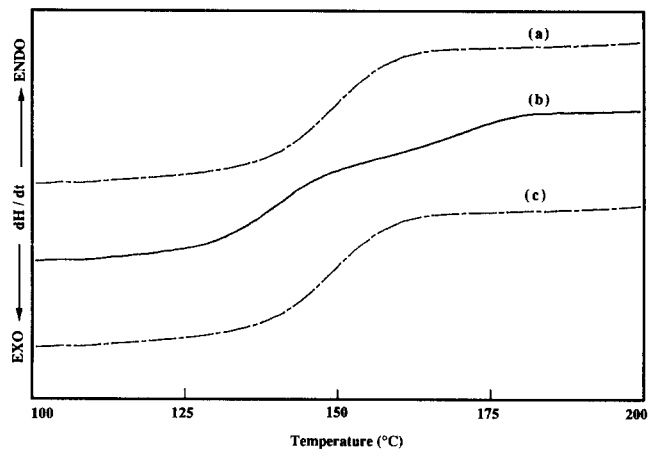

Figure 9 D.s.c. thermogram for TMPC/PS blend containing 40 wt% PS: (a) a second scan after first scan to erase prior thermal history; (b) transition behaviour after annealing at $T_1 = 255°C$ (*Figure 8*); (c) transition behaviour of 4th scan in *Figure 8*

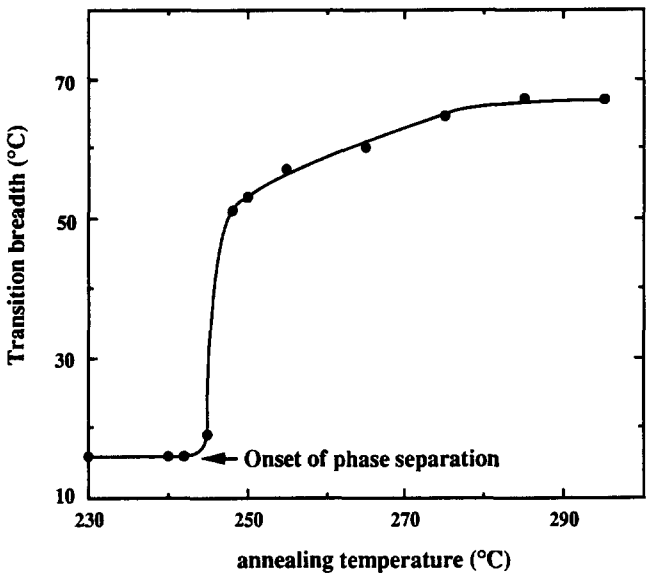

Figure 10 Change of transition breadth for a TMPC/PS blend containing 60 wt% PS as a function of annealing temperature (annealing time = 5 min)

true equilibrium phase boundary must lie between these limits. By successively repeating this process with other T_1 and T_2 values, the location of the phase boundary can in principle be narrowed to within any arbitrary temperature differential. However, this can be very time-consuming, so an alternative procedure was used to obtain the estimate of the equilibrium phase boundary shown as the lowest curve in *Figure 6*. Blends for each composition were isothermally annealed for 5 min at temperatures within the region of the expected phase boundary. After annealing, the samples were quenched and then scanned in the d.s.c. through the T_g region. The temperatures at which the onset and completion of the heat capacity changes occurred were noted and the breadth of the entire transition region was calculated and plotted versus the annealing temperature, as illustrated in *Figure 10*. The transition breadth remains relatively narrow so long as there is only one T_g; however, once the annealing temperature is high enough to induce phase separation, considerable broadening occurs. The onset of this broadening was taken as the phase separation temperature. The time of annealing can be adjusted to effectively remove any rate effects. The results obtained by this d.s.c. method are in good agreement with the phase separation temperature determined by light-scattering techniques[9].

Interaction energies

To extract information about interaction parameters from the experimental liquid–liquid phase boundary shown in *Figure 6*, two key assumptions are made. First, it is assumed that to a good approximation these data correspond to the spinodal curve. Secondly, it is assumed that the 'bare' interaction energy density, ΔP^*, does not depend on temperature, which amounts to saying that the temperature dependence of the Flory–Huggins parameter $B(T)$ stems entirely from compressibility effects. The validity of this assumption cannot be tested by only using the information presented here, so for now it must remain a postulate of this approach. For each blend composition, the phase separation temperature from *Figure 6* was used to calculate a ΔP^* from equation (15). While values from the d.s.c. method were used in this calculation, the choice of method makes a negligible difference in the calculation of ΔP^* owing to the relatively close agreement among the various data sets. The characteristic parameters for PS and TMPC shown in *Table 3* were used to calculate $\tilde{\rho}$ from the Sanchez–Lacombe equation of state and then ΔP^* was computed from equation (15). The values of ΔP^* so obtained are plotted as a function of composition in *Figure 11*. As seen, the ΔP^* values so obtained are effectively independent of blend composition and have a small negative value. Assuming that ΔP^* and the characteristic properties are not a function of temperature, B_{sc} can be calculated at any temperature from the ΔP^* shown in *Figure 11* by using equation (16). *Figure 11* compares the B_{sc} at 30°C calculated in this manner with the SANS experiments reported in the literature[7] for this system at 30°C. As expected for a miscible blend, the B_{sc} values obtained by both methods are negative over the entire range of composition. The absolute values from the two methods agree very well in the mid-composition range, i.e. around the critical composition. However, the composition dependence of the SANS values is much stronger than those calculated from ΔP^*. It is interesting to note that Sanchez and Balazs[16] have found the interaction energy computed from the spinodal calculation for the system PS–PVME is less composition-dependent than that calculated from SANS experiments. The origin or the meaning of this difference in composition dependence is not entirely clear at this point. One possible explanation may lie in our assumption that the experimentally determined phase-separation temperatures correspond to the spinodal curve. The error from this source will go to zero at the critical point. To bring the composition dependence of our calculated B_{sc} into line with that of SANS results would require a strongly composition-dependent ΔP^* and a strongly asymmetric deviation about the critical point of the observed phase separation temperatures from the spinodal line. An alternative possibility is that errors in the interaction energies obtained by the SANS technique have occurred. These SANS measurements were made in the glassy state so

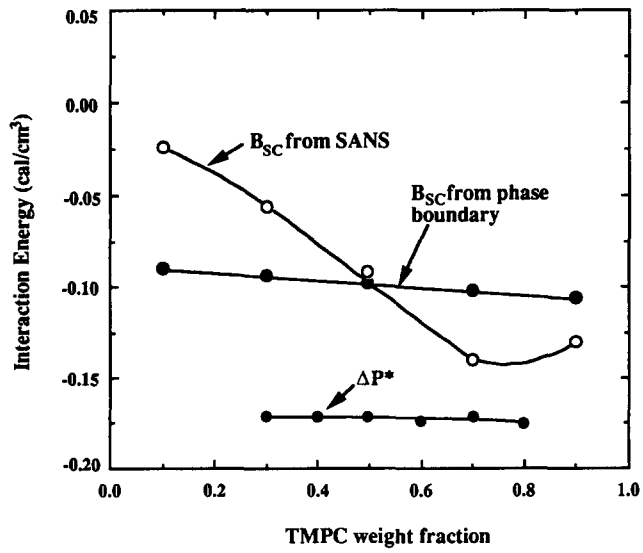

Figure 11 Composition dependence of the bare interaction parameter (ΔP^*) and B_{sc} (defined by equation (16)) obtained here with the B_{sc} from SANS experiments[7]

they reflect a non-equilibrium condition, the extent of which will depend on the distance from the glass transition temperature. Based on the observation on another system by Kramer and Sillescu[39], this effect could lead to an overestimate of the composition dependence. At this point, there is no simple way to distinguish among these or other possibilities.

The Flory–Huggins parameter $B(T)$ and its components B^h and $-TB^s$ can be calculated from equations (4), (13) and (14). *Figure 12* shows how they vary with temperature for a blend containing 50 wt% of PS, assuming that ΔP^* is not a function of temperature. The term B^h, which is related to the heat of mixing, becomes more negative as the temperature increases because of the predicted volume contraction on mixing. A negative excess volume for TMPC/PS blends has been reported[4,6]. The term $-TB^s$ becomes larger and more positive as temperature increases. This behaviour is in accord with the thermodynamic analysis by Sanchez[15,40], which argues that thermally induced phase separation is entropically driven. *Figure 13* shows how B_{sc} and the combinatorial entropy term in the spinodal condition change with temperature for a blend containing 50% by weight TMPC. Since $B(T)$ and B_{sc} depend on composition, their values are different, as illustrated in *Figures 12* and *13*. Using a fixed value of $\Delta P^* = -0.17$ cal cm^{-3}, the spinodal curve calculated from the equation of state and equation (15) agrees with the experimentally determined phase-separation temperature (*Figure 14*).

Atomic charge distributions for the blend components

One quantitative approach to modelling intermolecular interactions is to assign partial charges to each atom and then sum the dispersive and electrostatic contributions for each atom pair in the system. The latter is a formidable task beyond the scope of this paper; however, the former is relatively simple to do. Such information about charge distributions in each polymer repeat unit can serve as a useful guide about possible polar interactions between polymer pairs. The charge distributions for polystyrene, polycarbonate, and tetramethyl polycarbonate were

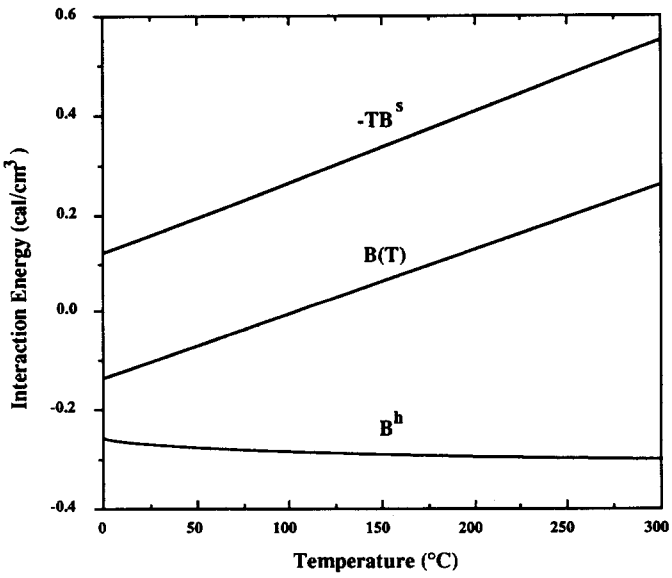

Figure 12 Temperature dependence of the extended Flory–Huggins interaction energy and its enthalpic and entropic components for a TMPC/PS blend containing 50 wt% PS

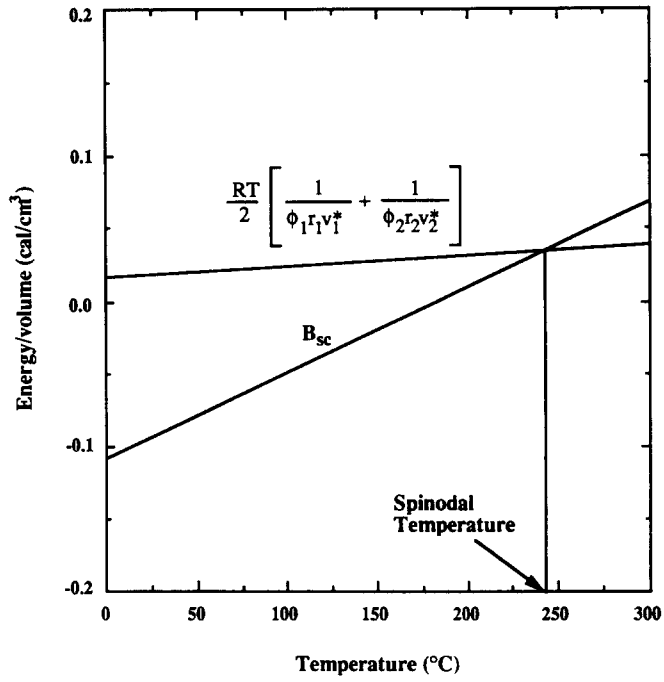

Figure 13 Effect of temperature on B_{sc} and the combinatorial entropy term in the spinodal condition (equations (15) and (16)) for a TMPC/PS blend containing 50 wt% PS: the interaction of the two lines gives the spinodal temperature

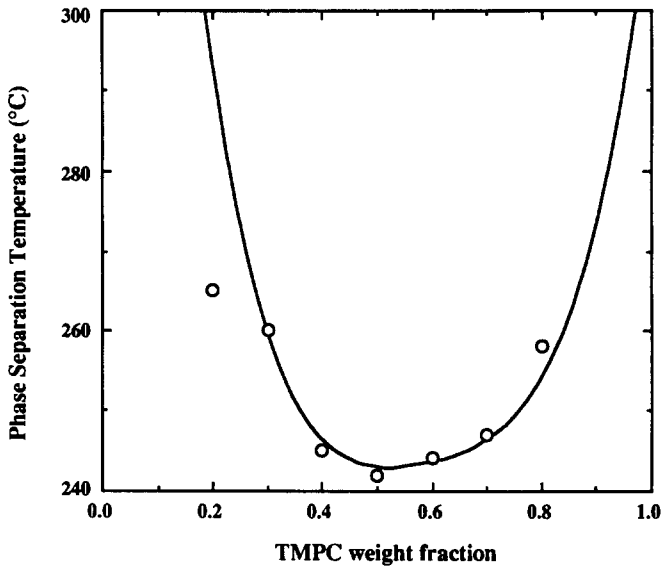

Figure 14 Comparison of the experimental phase separation temperatures (○) obtained by the d.s.c. method and with the predicted spinodal curve (——) by using the lattice fluid theory and $\Delta P^* = -0.17$ cal cm^{-3}

calculated by the Gast–Huck method using SYBYL Software from TRIPOS Associates Inc. with the results shown in *Figure 15*. In this approach, the Gasteiger–Marsili method[41,42] is used to calculate the σ-component of the atomic charge and the Hückel method[43] is used to calculate the π-component of the atomic charge. The total charge on each atom is the sum of these two calculated charges. It is clear that the electrostatic or polar interactions between PS and TMPC are not extremely strong as judged from examination of these atomic partial charges. This suggests that our assumption that the LCST behaviour for this system stems from

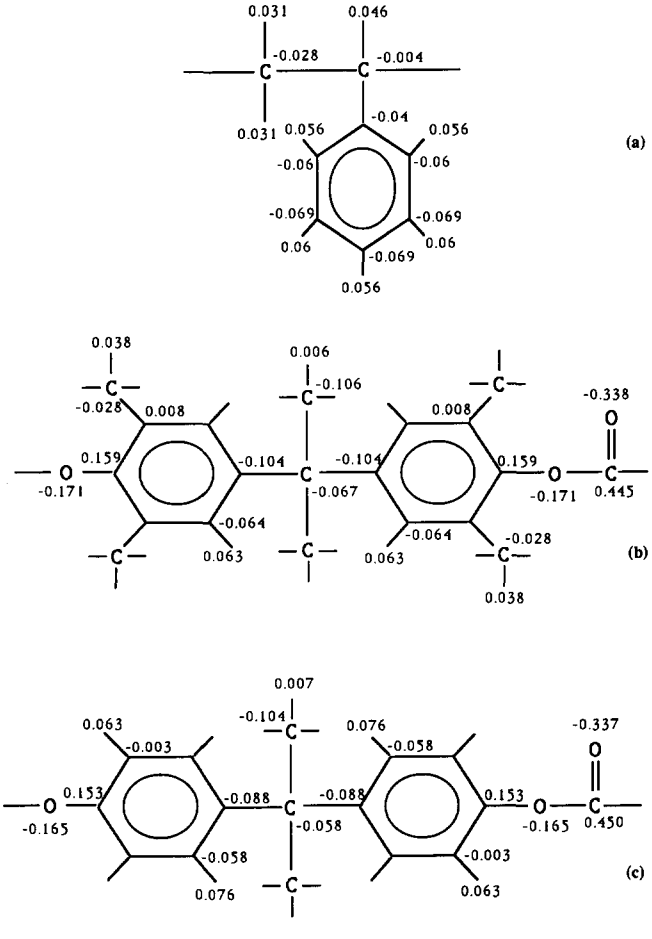

Figure 15 Atomic charge distribution for the repeat units of (a) PS, (b) TMPC, (c) PC calculated by the Gast–Huck method

equation of state contributions to the free energy rather than specific interactions may be reasonable. Indeed the interaction energy we calculate, i.e. $\Delta P^* = -0.17$ cal cm^{-3} is very small, but it is slightly negative, which leads to the miscibility observed. In the presence of strong specific or directionally sensitive interactions, even the blend interaction energy stripped of free volume contributions, i.e. ΔP^*, will become a strong function of temperature since thermal energy tends to randomize the orientation of chain segments, thus diminishing the number of favourable pair configurations[16,44].

It is interesting to compare the charge distribution of TMPC with that of polycarbonate because the latter evidently interacts endothermically with PS since this pair is not miscible. Since PS is also miscible with poly(2,6-dimethyl-1,4-phenylene oxide) or PPO, the key to the interaction that makes TMPC miscible with PS probably lies in that part of the TMPC structure that it is identical to PPO, i.e.

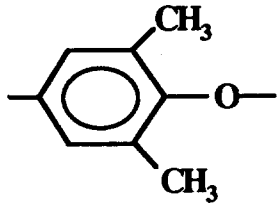

The most obvious effects of the methyl substitution are the further polarization of the rings, e.g. the charges on the 1 and 4 carbons go from −0.088 and 0.153 for PC to −0.104 and 0.159 for TMPC and the dipole formed by the bond connecting the ether oxygen to the ring carbon is further strengthened (the charges go from −0.165 and 0.153 to −0.171 and 0.159). There are, of course, some other changes as well. An assessment of the net effect caused by these redistributions will require a very detailed molecular simulation.

SUMMARY

The Sanchez–Lacombe equation of state theory of mixture has been applied to blends of polystyrene and tetramethyl polycarbonate. The characteristic equation of state parameters for the two homopolymers were obtained by fitting the model to experimental *PVT* data reported here. The temperatures at which blends of TMPC/PS phase separate were carefully determined and used to compute the Sanchez–Lacombe interaction parameter, ΔP^*. The latter was done by assuming the experimental phase boundary approximates the spinodal curve. The values of ΔP^* calculated in this way were found to be independent of blend composition within experimental errors. By further assuming that ΔP^* does not depend on temperature, the Sanchez–Lacombe theory was used to compute the Flory–Huggins and related interaction parameters as a function of temperature and composition. This allowed comparison with interaction parameters determined at 30°C[7] by small-angle neutron scattering, SANS. The values found here agreed very well with the SANS result near the blend critical composition, but were less composition-dependent than the SANS values. Possible reasons for the differences in composition dependence were discussed.

The assumption that ΔP^* is independent of temperature could not be critically evaluated from the information available. However, this assumption seems reasonable in light of the relatively weak interactions found for this system and calculations of atomic charges for the component polymers. A test of the utility of this approach to evaluation of interaction parameters will be described in further papers that deal with miscibility behaviour of copolymers based on styrene and on tetramethyl polycarbonate.

ACKNOWLEDGEMENT

This research was sponsored by the National Science Foundation Grant No. DMR-89-00704 administered by the Polymer Program. The authors wish to thank Professor I. C. Sanchez for his valuable assistance and advice.

REFERENCES

1 Shaw, M. T. *J. Appl. Polym. Sci.* 1974, **18**, 449
2 Casper, R. and Morbitzer, L. *Makromol. Chem.* 1977, **58/59**, 1
3 Humme, G., Rohr, H. and Serini, V. *Makromol. Chem.* 1977, **58/59**, 85
4 Yee, A. F. and Maxwell, M. A. *J. Macromol. Sci.–Phys.* 1980, **17**, 543
5 Wisniewsky, C., Marin, G. and Monge, P. *Eur. Polym. J.* 1984, **7**, 691
6 Fernandes, A. C., Barlow, J. W. and Paul, D. R. *Polymer* 1986, **27**, 1789
7 Yang, H. and O'Reilly, J. M. *Mater. Res. Soc. Symp. Proc.* 1987, **79**, 129

8 Brereton, M. G., Fisher, E. W. and Herkt-Maetzky, C. *J. Chem. Phys.* 1987, **10**, 6144
9 Guo, W. and Higgins, J. S. *Polymer* 1990, **31**, 699
10 Fernandes, A. C., Barlow, J. W. and Paul, D. R. *Polymer* 1986, **27**, 1799
11 Min, K. E. and Paul, D. R. *Macromolecules* 1987, **20**, 2828
12 Sanchez, I. C. and Lacombe, R. H. *J. Phys. Chem.* 1976, **80**, 2352
13 Sanchez, I. C. and Lacombe, R. H. *J. Polym. Sci., Polym. Lett. Edn.* 1977, **15**, 71
14 Sanchez, I. C. and Lacombe, R. H. *Macromolecules* 1978, **11**, 1145
15 Sanchez, I. C. 'Encyclopedia of Physical Science and Technology' Vol. XI, Academic Press, New York, 1987, p. 1
16 Sanchez, I. C. and Balazs, A. C. *Macromolecules* 1989, **22**, 2325
17 Flory, P. J. *J. Chem. Phys.* 1942, **10**, 51
18 Huggins, M. L. *J. Chem. Phys.* 1941, **9**, 440
19 Paul, D. R., Barlow, J. W. and Keskkula, H. 'Encyclopedia of Polymer Sci. and Engng.' 2nd Edn., Vol. 12, 1988, p. 399
20 Sanchez, I. C. *Polymer* 1989, **30**, 471
21 Flory, P. J. *J. Am. Chem. Soc.* 1965, **87**, 1831
22 Eichinger, B. E. and Flory, P. J. *Trans. Faraday Soc.* 1968, **64**, 2035
23 Simha, R. *Macromolecules* 1977, **10**, 1025
24 Panayiotou, C. G. *Macromolecules* 1987, **20**, 861
25 Patterson, D. and Robard, A. *Macromolecules* 1978, **11**, 690
26 Sanchez, I. C. *Macromolecules* 1991, **24**, 908
27 Quach, A. and Simha, R. *J. Phys. Chem.* 1972, **76**, 416
28 Quach, A., Wilson, P. S. and Simha, R. *J. Macromol. Sci.–Phys.* 1974, **B9**(3), 533
29 Zoller, P. *J. Polym. Sci., Polym. Phys. Edn.* 1982, **20**, 1453
30 Quach, A. and Simha, R. *J. Appl. Phys.* 1971, **42**, 4592
31 Zoller, P. *J. Polym. Sci., Polym. Phys. Edn.* 1978, **16**, 1261
32 Boyer, R. F. *Macromolecules* 1982, **15**, 774
33 Richardson, M. J. and Savill, N. G. *Polymer* 1977, **18**, 3
34 Simha, R., Wilson, P. S. and Olabisi, O. *Kolloid-Z. Z. Polym.* 1973, **251**, 402
35 Zoller, P. *J. Polym. Sci., Polym. Phys. Edn.* 1980, **20**, 157
36 Dee, G. T. and Walsh, D. J. *Macromolecules* 1988, **21**, 811
37 Sanchez, I. C. 'Polymer Blends' (Eds D. R. Paul and S. Newman), Vol. 1, Academic Press, New York, 1978, Ch. 3
38 Nishimoto, M., Keskkula, H. and Paul, D. R. *Polymer* 1991, **32**, 272
39 Kramer, E. J. and Sillescu, H. *Macromolecules* 1989, **22**, 414
40 Sanchez, I. C. 'Polymer Compatibility and Incompatibility Principles and Practices' (Ed. K. Solcz), MMI Press Symposium Series 2, Harwood Academic Publishers, New York, 1982, p. 59
41 Gasteiger, J. and Marsili, M. *Tetrahedron* 1980, **36**, 3219
42 Gasteiger, J. and Marsili, M. *Organ. Magn. Reson.* 1981, **15**, 353
43 Streitwieser, A. 'Molecular Orbital Theory for Organic Chemists', Wiley, New York, 1961
44 ten Brinke, G. and Karasz, F. E. *Macromolecules* 1984, **17**, 815